Bull Volcanol (2013) 75:696
DOI 10.1007/s00445-013-0696-3

RESEARCH ARTICLE

The nature and formation of cristobalite at the Soufrière Hills volcano, Montserrat: implications for the petrology and stability of silicic lava domes

Claire J. Horwell · Ben J. Williamson · Edward W. Llewellin · David E. Damby · Jennifer S. Le Blond

Received: 12 May 2012 / Accepted: 31 January 2013 / Published online: 21 February 2013

Abstract Cristobalite is commonly found in the dome lava of silicic volcanoes but is not a primary magmatic phase; its presence indicates that the composition and micro-structure of dome lavas evolve during, and after, emplacement. Nine temporally and mineralogically diverse dome samples from the Soufrière Hills volcano (SHV), Montserrat, are analysed to provide the first detailed assessment of the nature and mode of cristobalite formation in a volcanic dome. The dome rocks contain up to 11 wt.% cristobalite, as defined by X-ray diffraction. Prismatic and platy forms of cristobalite, identified by scanning electron microscopy (SEM), are commonly found in pores and fractures, suggesting that they have precipitated from a vapour phase. Feathery crystallites and micro-crystals of cristobalite and quartz associated with volcanic glass, identified using SEM-Raman, are interpreted to have formed by varying amounts of devitrification. We discuss mechanisms of silica transport and cristobalite formation, and their implications for petrological interpretations and dome stability. We conclude: (1) that silica may be transported in the vapour phase locally, or from one part of the magmatic system to another; (2) that the potential for transport of silica into the dome should not be neglected in petrological and geochemical studies because the addition of non-magmatic phases may affect whole rock composition; and (3) that the extent of cristobalite mineralisation in the dome at SHV is sufficient to reduce porosity—hence, permeability—and may impact on the mechanical strength of the dome rock, thereby potentially affecting dome stability.

Keywords Cristobalite · Quartz · Soufrière Hills, Montserrat · Lava dome · Vapour-phase silica

Editorial responsibility: E.S. Calder

C. J. Horwell (✉) · D. E. Damby
Institute of Hazard, Risk and Resilience, Department of Earth Sciences, Durham University, Science Labs., South Road, Durham DH1 3LE, UK
e-mail: claire.horwell@durham.ac.uk

B. J. Williamson
Camborne School of Mines, College of Engineering, Mathematics and Physical Sciences, University of Exeter, Cornwall Campus, Penryn TR10 9EZ, UK

B. J. Williamson · J. S. Le Blond
Department of Earth Sciences, Natural History Museum, Cromwell Road, London SW7 5BD, UK

E. W. Llewellin
Department of Earth Sciences, Durham University, Science Labs., South Road, Durham DH1 3LE, UK

J. S. Le Blond
Brighton and Sussex Medical School, Falmer, Brighton, East Sussex BN1 9PX, UK

Introduction

The crystalline silica (SiO_2) polymorphs cristobalite, quartz and, to a lesser extent, tridymite are common components of lava domes at basaltic–andesitic to rhyolitic volcanoes, e.g. Soufrière Hills volcano (SHV), Montserrat (Baxter et al. 1999; Williamson et al. 2010), Unzen, Japan (Nakada and Motomura 1999), Mt. St. Helens (MSH), USA (Blundy and Cashman 2001; Pallister et al. 2008), Merapi, Indonesia (Damby et al. 2013) and Chaitén, Chile (Horwell et al. 2010). Quartz in dome rocks may be magmatic in origin or may have precipitated from hydrothermal fluids. Cristobalite and tridymite are mainly found in pores and fractures and are thus interpreted as vapour-phase

precipitates (Baxter et al. 1999; de Hoog et al. 2005). At SHV, cristobalite is also thought to form by devitrification, i.e. by solid-state crystallisation from amorphous volcanic glass (Baxter et al. 1999; Murphy et al. 2000); however, no direct evidence for this mode of formation has been presented. Cristobalite is also found as a hydrothermal product at some volcanoes (e.g. Mt. Augustine; Getahun et al. 1996) and in ignimbrite and tuff deposits (e.g. Stimac et al. 1996; Yurtmen and Rowbotham 1999) and is closely associated with K-feldspar within spherulites in devitrified obsidian domes and rhyolitic lavas (e.g. Swanson et al. 1989; Dadd 1992). The cristobalite stability field is between 1,470 and 1,713 °C at <1 GPa (Deer et al. 1996); hence, it exists as a metastable phase in dome-forming volcanic systems, where temperatures are typically ≤850 °C. Its persistence at ambient temperature and pressure is due to the considerable activation energy required for the reconstructive transformation of cristobalite to low-quartz (Deer et al. 1996).

Dome-collapse events of SHV produce volcanic ash rich in cristobalite (up to ~25 wt.%; Baxter et al. 1999; Horwell et al. 2003; Horwell et al. 2010; Baxter et al. Accepted; Horwell et al. 2013). The ash plumes produced by pyroclastic density currents (PDCs) resulting from these dome-collapse events (known as co-PDC ash fall) show notable cristobalite enrichment in the very-fine particle fraction (sub-2 μm; Horwell et al. 2003), probably as a result of size and density fractionation during fragmentation of dome rock within PDCs (Horwell et al. 2001). The presence of abundant sub-2 μm cristobalite particles in the ash may present a potential respiratory health risk to exposed populations (Horwell and Baxter 2006).

The aims of the current study are to determine the nature and mode of formation of cristobalite in the Soufrière Hills volcanic dome. We consider the nature of cristobalite formation through scanning electron microscopy (SEM) with Raman spectroscopy, energy dispersive X-ray spectrometry (EDS) and cathodoluminescence (CL) and by X-ray diffraction (XRD) and X-ray fluorescence (XRF). The work builds on that of Baxter et al. (1999) who showed, for the first time, that cristobalite forms in the Soufrière Hills dome lava and is sufficiently abundant in the resultant dome-collapse co-PDC ash fall to be a respiratory health hazard. Further to this, Baxter et al. (1999) suggest that the cristobalite is formed by vapour-phase crystallisation and devitrification, based on observations of groundmass silica phases as vesicle infills and fine-grained patches within interstitial glass. Here, we identify textural criteria by which these modes of formation can be inferred for individual cristobalite crystals in the dome rocks and ash. The use of SEM-Raman allows definitive confirmation of the silica polymorph of crystals and micro-patches of SiO_2 (identified by SEM-EDS). The results have implications for studies of dome stability in terms of assessing micro-structural evolution in response to vapour-phase mineralisation and promote consideration of the consequences of sub-solidus redistribution of silica for the interpretation of whole-rock geochemical data.

Active lava domes are inherently unstable, and partial or complete dome collapse poses a major hazard to local communities. This has motivated extensive research into the mechanisms of dome failure (Calder et al. 2002), with work focussing on collapse triggers, such as pressurisation of gas within the dome (Voight and Elsworth 2000; Elsworth and Voight 2001), heavy rainfall (Matthews et al. 2002; Elsworth et al. 2004), slope over-steepening (Sparks et al. 2000) and hydrothermal weakening of the dome (Edmonds et al. 2003). In this study, we propose a new hypothesis, based on our observations of the distribution of vapour-phase minerals: that vapour-phase mineralisation also plays an important role in dome stability via two opposing and thus competing processes: (1) The occlusion of pore space by vapour-phase precipitates could lead to a reduction in permeability, promoting gas pressurisation and subsequent destabilisation of the dome; (2) Mineralisation could cement and densify the dome, stabilising the edifice.

The presence of cristobalite that has precipitated from a vapour phase in dome rocks is evidence that silica is redistributed within the magmatic system. We propose two hypotheses for the transport mechanism: (1) Silica redistribution may occur locally (over the length-scale of individual vugs) as a result of leaching of volcanic glass and other phases adjacent to pore spaces, potentially mediated by HF and other acid solutions/vapours. In this scenario, which we refer to as 'local redistribution', the bulk SiO_2 content of dome rock is not affected. (2) Alternatively, or additionally, silica may be transported into the dome from magmatic gases below the dome or from sources outside the magmatic system, such as connate or meteoric waters incorporated via hydrothermal convection. In this scenario, which we refer to as 'bulk transport', the bulk SiO_2 content of dome rock is increased, implying that the whole-rock geochemical composition of a dome rock sample may not be the same as that of the magma from which it crystallised.

Cristobalite formation mechanisms

Rogers (1922) and Larsen et al. (1936) were the first to postulate that cristobalite can form in cavities in volcanic rocks as a consequence of the supply of silica by steam. This hypothesis has been supported by more recent work (described below), and there is now evidence that the transport of Si could be mediated by a number of different phases at temperatures and pressures appropriate for the conduit/dome system (the SHV dome is thought to be around 300 m thick (Watts et al. 2002), corresponding to a pressure of around 7 MPa (650–830 °C) at its base (Hicks et al. 2009 and references therein)):

Si- and F-bearing fluids

Churakov et al. (2000) identified ten silica-carrying gas species in volcanic systems. They found through thermodynamic modelling that, at >950 °C, Si in the gas phase is transported as SiO and SiO_2, with SiO being more prevalent at higher temperatures. Between 900 and 950 °C, $SiOF_2$, SiF_4, SiO and SiO_2 species play an equal role in Si transport. Below 900 °C, in the temperature range of the SHV dome, SiF_4 species prevail. Geochemical modelling also supports the theory that Si can be transported as SiO gas at temperatures >700 °C (0.1 MPa) (Korzhinsky et al. 1995). Formation of cristobalite from SiO is also suggested by Reich et al. (2009), who propose that amorphous glass may convert to SiO in the presence of a reducing agent (such as CO); however, they invoke this mechanism in an eruption column rather than in a lava dome. Thermodynamic modelling by de Hoog et al. (2005) confirmed that, upon degassing, magmatic SiF_4 gas will react with water to form vapour-phase silica in volcanic systems:

$$SiF_4(g) + 2H_2O(g) \leftrightarrow SiO_2(s) + 4HF(g). \quad (1)$$

The reaction equilibrium is strongly dependent on temperature, pressure and HF fugacity (White and Hochella 1992; de Hoog et al. 2005); hence, depending on ambient conditions, silica may be deposited (reaction moves to the right), or corroded by HF (reaction moves to the left).

Cl-bearing fluids

Foustoukos and Seyfried (2007) have conducted experiments on quartz solubility in Cl-bearing aqueous vapour fluids (at 365–430 °C, 21.9–38.1 MPa) and found that they can contain significant concentrations (from 2.81 to 14.6 mmol kg^{-1}) of dissolved SiO_2. Shmulovich et al. (2006) determined that the main species for the transport of Si at temperatures <750 °C (0.1 MPa) is likely to be $SiCl_4$ gas. The temperatures in these experiments are too low for deep dome conditions; however, elevated concentrations of HCl and HF gases have been measured at the crater's edge from the Soufrière Hills dome (533 and 22 ppbv, respectively; Allen et al. 2000). The HF/HCl gas ratio of 0.004 reported by Allen et al. (2000) suggests that $SiCl_4$ could be the dominant Si-bearing phase, with SiO and SiF_4 playing a subordinate role, if Cl-bearing fluids could support silica at higher temperatures.

Kinetic and thermodynamic constraints control the silica polymorph (or amorphous phase) that precipitates from a vapour. Renders et al. (1995) measured the rates of precipitation for cristobalite at 150–300 °C from $Si(OH)_4$ solution and found that cristobalite forms only where silica concentrations are above the cristobalite silica saturation limit but less than the amorphous silica saturation limit; crucially, they also found that there have to be cristobalite nuclei present. Jones and Segnit (1972) hypothesised that, if cristobalite nuclei are present in a hydrothermal environment, the epitaxial crystallisation of cristobalite requires less energy than re-arrangement of the cristobalite substrate to form quartz. These findings imply that, in the volcanic system, the formation of cristobalite by devitrification may be a necessary precursor to the formation of vapour-phase cristobalite, in order to provide the required nuclei.

Background to the Soufrière Hills volcano

Soufrière Hills, Montserrat, is an active, andesitic, dome-forming volcano in the Lesser Antilles Island Arc (see review in Druitt et al. 2002). The current eruption began in July 1995 with a series of phreatic explosions. This was followed by a period of dome growth from mid-November with the first major collapse occurring in April 1996. Since then, there have been intermittent cycles of effusive dome building and collapse, often closely followed by a period of Vulcanian explosive eruptions. To date, there have been five phases of dome growth, accompanied by significant pauses defined by residual activity (rockfalls, degassing and low levels of seismicity) (Wadge et al. 2013). At the time of writing (November 2012), SHV is still active; however, the last major dome collapse occurred in February 2010.

Sample selection

Nine samples of dome rock were acquired from the archives of the Montserrat Volcano Observatory (MVO) in June 2006. Sub-samples are currently held within the collections of the Natural History Museum, London. Sample numbers and a summary of sample properties are given in Table 1, along with information on eruption date and type and phase of dome growth.

The dome rocks were originally sampled from PDC (block-and-ash flow) deposits. The samples chosen spanned the current eruption (1995 onwards) and encompass a range of ages and densities of dome rock (vesicular to dense). They likely cover a range of sources, from shallow dome material to deeper dome/upper conduit, and dome residence times. Information on the sample history was obtained from the MVO sample database, but no information was available on the location, depth or residence time of each sample within the dome complex prior to collapse.

Where multiple samples from the same flow were available within the MVO archives, representative blocks were chosen with the help of MVO staff. It is noted, however, that the nine samples cannot be fully representative of the collapsed lobes of lava, given the heterogeneous nature of the dome and the PDCs.

Two samples were chosen which predate the current eruptive period (i.e. pre-1995). The oldest sample (MVO819) is

Table 1 Sample summary and crystalline silica features observed

Sample no.	Date of collapse/ eruption	Phase of dome growth[c]	Date of collection	Description	Information	Prismatic	Platy	Devit. cristob.	Devit. quartz
MVO819 BM.2007, P1(11)	174 k.a. BP		15/2/98	Dome lava; very dense, grey/brown	Ancient sample from old complex	✓ But rare	✓	✓	✓
MVO945 BM.2007,P1(12)	400 a. BP		?	Dome lava; dense, red/brown	Ancient sample from Castle Peak	✓	✗	✗	✓
MVO287 BM.2007,P1(2)	21/9/97	1	21/9/97	Juvenile block; vesicular; light grey	From dome collapse deposit	✓	✗	✓	✗
MVO288 BM.2007,P1(3)	21/9/97	1	21/9/97	Juvenile block; frothy, light grey	From dome collapse deposit	✓ but rare	✗	✗	✗
MVO617 BM.2007,P1(9)	21/9/97	1	16/5/98	Dome lava; Dense; green/ dark grey	From dome collapse deposit	✓	✗	✓	✗
MVO332 BM.2007,P1(8)	26/12/97	1	4/1/98	Dome lava; vesicular; pale grey	From 'Boxing Day' collapse deposit	✓	✗	✓	✗
MVO1236 BM.2007,P1(18b)	12/7/03	2	1/8/03– 15/11/03?	Dome lava; dense; pale grey	From dome collapse deposit (full collapse)	✓	✓	✓	✓
MVO1406 BM.2007,P1(24)	20/5/06	3	?	Dome lava; dense; pale grey	From dome collapse deposit	✓	✗	✓	✗
MontR1[a] BM.2007,P2(1)	20/5/06	3	22/6/06	Dome lava, dense, red	From dome collapse deposit	✓	✓	✗	✓
MVO244[b]	5/8/97	1	6/8/97	Large pumice block	Erupted during Vulcanian explosion	–	–	–	–
MVO289[b]	25/9/97	1	25/9/97	Juvenile pumice flow block	Erupted during Vulcanian explosion	–	–	–	–
MVO291[b]	29/9/97	1	29/9/97	Airfall pumice clast	Erupted during Vulcanian explosion	–	–	–	–
MVO374[b]	Sept/Oct 1997	1	23/12/97	Pumice	Erupted during Vulcanian explosion	–	–	–	–

[a] Collected by BW from deposit rather than archive

[b] Samples supplied by Prof. Steve Sparks, University of Bristol

[c] Dome growth phase defined by Wadge et al. 2013

from the ancient SHV, dated by Harford et al. (2002) using $^{40}Ar/^{39}Ar$, at 174±3 kaB.P. Sample MVO945 is from the seventeenth century eruption of the Castle Peak lava dome (part of the Soufrière Hills dome complex) (MVO, pers. comm.).

Three samples of rock were collected from the block-and-ash flow deposits resulting from the large dome-collapse (21 September 1997) which immediately preceded the onset of Vulcanian explosions. Sample MVO617 is a sample of dense dome rock; sample MVO287 is a moderately vesicular sample containing fractured phenocrysts and burst melt inclusions (described in detail in Williamson et al. (2010)); sample MVO288 is even more vesicular, showing pumiceous textures.

One sample (MontR1) was collected in June 2006 from the block-and-ash flow deposits from the 20 May 2006 dome collapse event. MVO1236 and MVO1406 are samples of dense dome rock collected from the block-and-ash flows generated by the collapses of 12 July 2003 and 20 May 2006, respectively. MVO332 is a sample of moderately vesicular dome rock collected following the lateral blast and collapse of the lava dome on 26 December 1997.

For comparative purposes, we also characterised pumice erupted during Vulcanian explosions at Soufrière Hills (August–October 1997, provided by Prof. R.S.J. Sparks, University of Bristol). These samples (MVO244, MVO289,

MVO291 and MVO374) provide an effective control because they should be unaffected by secondary mineralisation.

Methods

Imaging of vapour-phase minerals

Imaging was carried out at the Natural History Museum (NHM), London, on both rough chips of dome rock (~0.5 cm in diameter; Au (95 %)/Pd (5 %) coated) and as carbon-coated polished thin sections. High-resolution images were obtained using a Philips XL-30 field emission scanning electron microscope. Lower magnification back-scattered electron (BSE) images were obtained using a LEO 1455 Variable Pressure SEM with Oxford Instruments INCA energy dispersive X-ray analysis system (SEM-EDS). Colour (RGB) CL images, with complementary BSE images and EDS maps, were obtained using an EVO® LS 15 (20 kV, 10 nA) with a Gatan ChromaCL™ detector and DigiScan™ beam control system.

Mineralogical characterisation of vapour-phase minerals

To distinguish cristobalite from tridymite and quartz, uncoated polished sections were analysed using a Renishaw SEM-Raman Structural and Chemical Analyser which couples simultaneous Raman spectroscopy (inVia microscope, laser spot size 1.2 μm, 785 nm wavelength) with variable-pressure SEM-EDS (Jeol JSM-6060 LV SEM with Oxford Instruments INCA energy dispersive X-ray analysis) at Renishaw plc, UK. This allowed the imaging and identification of individual crystals of silica polymorphs. Reference spectra, used in the identification of silica polymorphs, were obtained from the online Handbook of Minerals Raman Spectra (http://www.ens-lyon.fr/LST/Raman/index.php, which uses reference spectra from Kingma and Hemley 1994).

Quantification of silica polymorph concentrations in dome rock

The proportions of the different silica polymorphs in the dome rock samples (cristobalite, quartz and tridymite) were determined by XRD using an Enraf-Nonius XRD (with Cu$K_{\alpha 1}$ radiation) with an INEL curved 120 °2θ position-sensitive detector (PSD) at the NHM, London. We followed the Internal Attenuation Standard (IAS, in this case using ZnO) method of Le Blond et al. (2009), which allows rapid quantification of single mineral phases in heterogeneous powders without prior knowledge of the mineral assemblage. The rocks were first powdered to approximately <20 μm using an agate pestle and mortar. Tube operating conditions were 45 kV and 45 mA, using horizontal and vertical slits set at 0.24×5.0 mm. NBS silicon and silver behenate were used as external 2θ calibration standards.

Whole-rock geochemical analysis of dome rocks

Dome rock and pumice samples were crushed and ground using an agate pestle and mortar. Major elements were determined on fused glass beads prepared using ignited powders mixed with 100 % Li tetraborate flux, with a sample to flux ratio of 1:30. The samples were analysed using a PANalytical Axios Advanced XRF spectrometer at the Department of Geology, University of Leicester, UK, to determine major-element oxides.

Results

Nature of crystalline silica phases in dome samples

Five different forms of crystalline silica were identified in the Soufrière Hills dome rock through imaging and analysis of dome-rock samples by SEM-EDS and SEM-Raman, which are detailed below:

Quartz phenocrysts These primary magmatic phenocrysts, between 300 and 1,000 μm max axis diameter, are often rounded and embayed (Fig. 1a). These are found in most samples but are not common, typically fewer than two or three phenocrysts in a standard polished section.

Prismatic cristobalite These crystals are between 20 and 50 μm max axis diameter. In polished section, the prismatic cristobalite (identified using SEM-Raman (Fig. 2a)) has characteristic 'fish-scale' cracks (Fig. 1b and c), which results from a 5 % decrease in volume from the displacive transition from ß to α cristobalite during cooling through ~240 °C (Carpenter et al. 1998). Prismatic cristobalite is observed in all samples of dome rock, including a few crystals in MVO288 (the pumiceous sample from the 21 Sept 1997 dome-collapse deposit). The prismatic cristobalite often appears to have either grown directly from the glassy vug wall (Figs. 1c and 3b–d) or sits on a crust of small (<5 μm diameter) plagioclase feldspar crystals (Fig. 3a, e and f) within the vesicle. In polished section, the fish-scale cristobalite is also seen as patches within the groundmass of dense dome rock (Fig. 1d).

The more vesicular samples allow direct observation into open cracks and pore spaces, which enabled the observation of cristobalite crystal morphology. The cristobalite crystals often appear to have cubic or tetragonal habit (Fig. 3a) and frequently display multiple twinning (Fig. 3b–f).

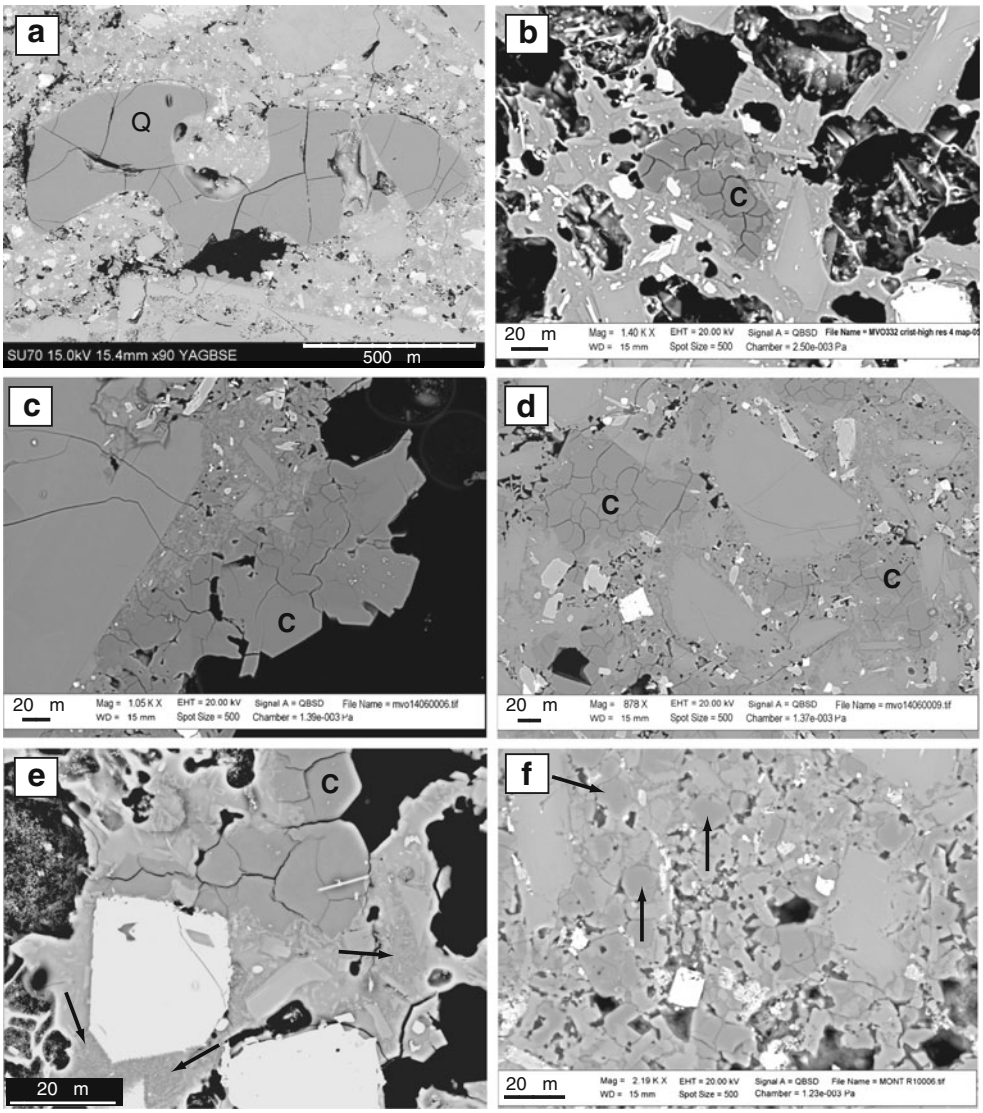

Fig. 1 Backscattered electron images showing dome rock morphology in thin section. **a** Quartz phenocryst (*Q*) in MVO617; **b** cristobalite crystal showing typical fish-scale cracking (*C*) in MVO332; **c** cristobalite crystals (*C*) protruding into open pore space in MVO1406. Note that the cristobalite and groundmass appear to merge; **d** cristobalite (*C*) apparently filling available void spaces in MVO1406; **e** 'Feathery' groundmass texture (indicated by *arrows*) in MVO287; **f** MontR1 groundmass appears completely devitrified with quartz (*dark grey*, indicated by *arrows*) and plagioclase feldspar (*lighter grey*) crystallites

Platy cristobalite The plates were confirmed as cristobalite (as opposed to tridymite) by SEM-Raman (Fig. 2b) and were observed growing into pore spaces in polished sections (where they appeared acicular, Fig. 4a and b) and in rough chips (Fig. 4c and d); the crystals appear to be hexagonal (Fig. 4 and d), although they could also be extremely flattened cubic or tetragonal forms (Fig. 4a and b). The crystals look very similar to those of hexagonal β-tridymite and may be paramorphs after this phase. The platy crystals were particularly common in MVO1236 (12 July 2003 collapse, dense dome lava), MontR1 (20 May 2006 collapse, dense dome lava) and MVO819 (177 ka B.P., dense dome lava).

Feathery crystalline silica in glass Within the glassy groundmass of most of the dome rock samples 'feathery' textures of poorly formed crystallites were observed (Fig. 1e). Individual patches are on a scale of <1–3 μm and are too small to be confidently identified by spot analysis with SEM-EDS, SEM-Raman or electron microprobe. Instead, the presence of micro-silicas in the volcanic glass was confirmed by carrying out a combination of BSE imaging, X-ray elemental mapping, CL imaging and SEM-Raman (of an area of partially devitrified glass) (Fig. 5a–d). Figure 5a shows an area of partially devitrified glass, labelled 'D', which contains plagioclase microlites and a phase with a BSE signal darker than the glass (labelled 'G') but similar to that of the cristobalite ('C'). The X-ray elemental map in Fig. 5b demonstrates that area 'D' is composed of plagioclase microlites (containing relatively abundant Al (green)) in a groundmass dominated by Si (blue) but with less K (red) than surrounding glassy areas. The dominance of blue indicates a Si-enriched area where glass is not the principal matrix phase. The CL signal is similar to that of the 'prismatic cristobalite' (type 2, Fig. 5c), although quartz can also show a similar colour (Boggs et al. 2002). Ultimately, the darker groundmass phase (by SEM-BSE) was confirmed as cristobalite using SEM-Raman, which gave a broad, curved background pattern, typical of amorphous glass, with peaks that match the

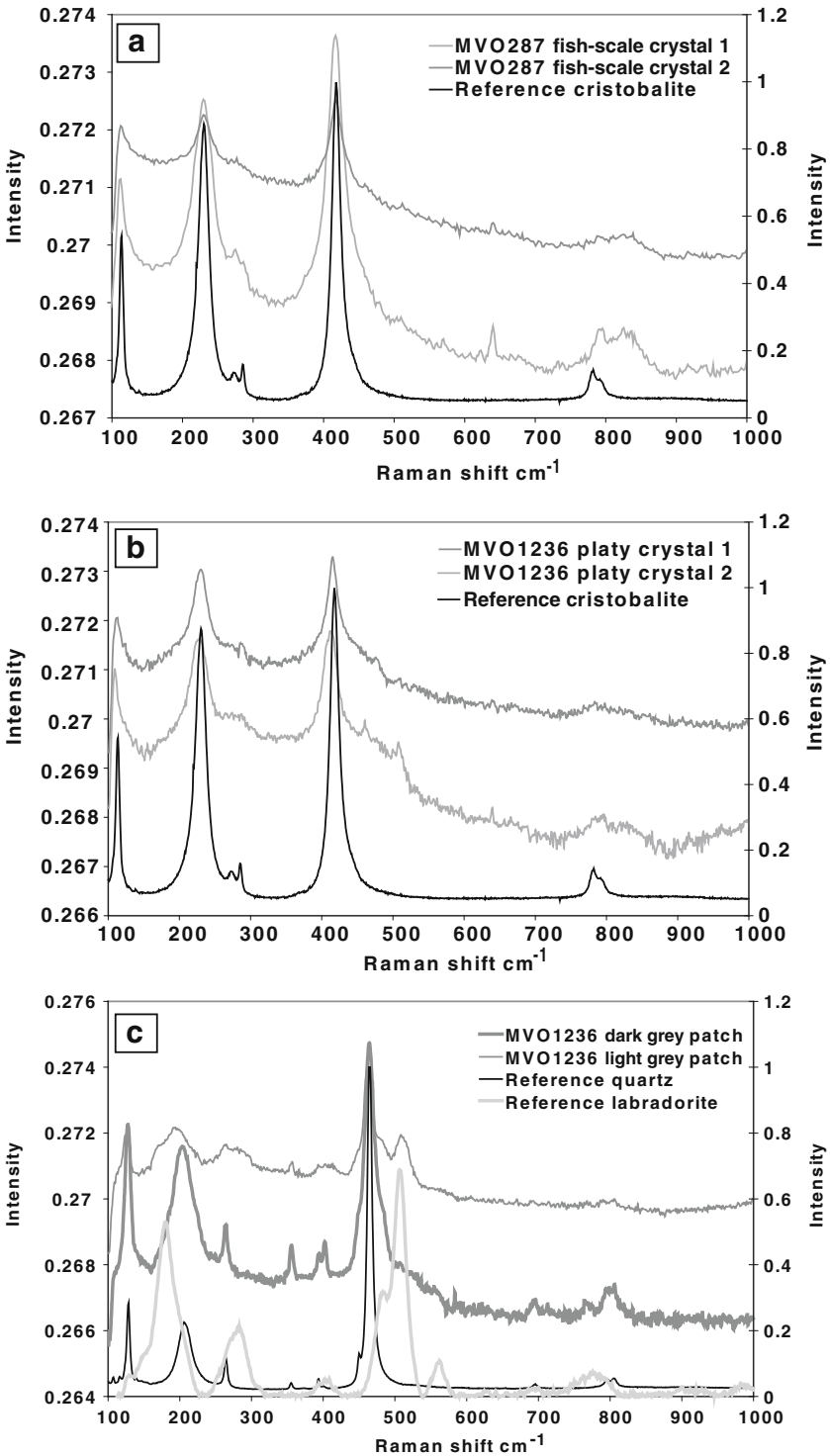

Fig. 2 Raman spectra. **a** Spectra for two fish-scale crystals in sample MVO287 with reference spectrum for cristobalite; **b** spectra for two platy crystals in sample MVO1236 with reference spectrum for cristobalite; **c** spectra for light-grey and dark-grey patches in the groundmass of MVO1236 with reference spectra for quartz and labradorite

reference patterns for both cristobalite and plagioclase (labradorite) (Fig. 5d). Quartz was not detected in these patches by SEM-Raman.

Quartz microlites Four of the samples (MontR1, MVO819, MVO945 and MVO1236) had areas which were glass-free, and the groundmass was composed entirely of microlites (<100 μm diameter) including ~10 μm diameter patches of subhedral silicas (indicated by arrows in Fig. 1f) confirmed to be quartz by SEM-Raman (Fig. 2c). These patches are found in MontR1, MVO945 and MVO1236 (note that cristobalite patches showing fish-scale cracking are still present in original pore spaces in these samples, Fig. 1f). In association with these forms are lighter grey, more lath-shaped

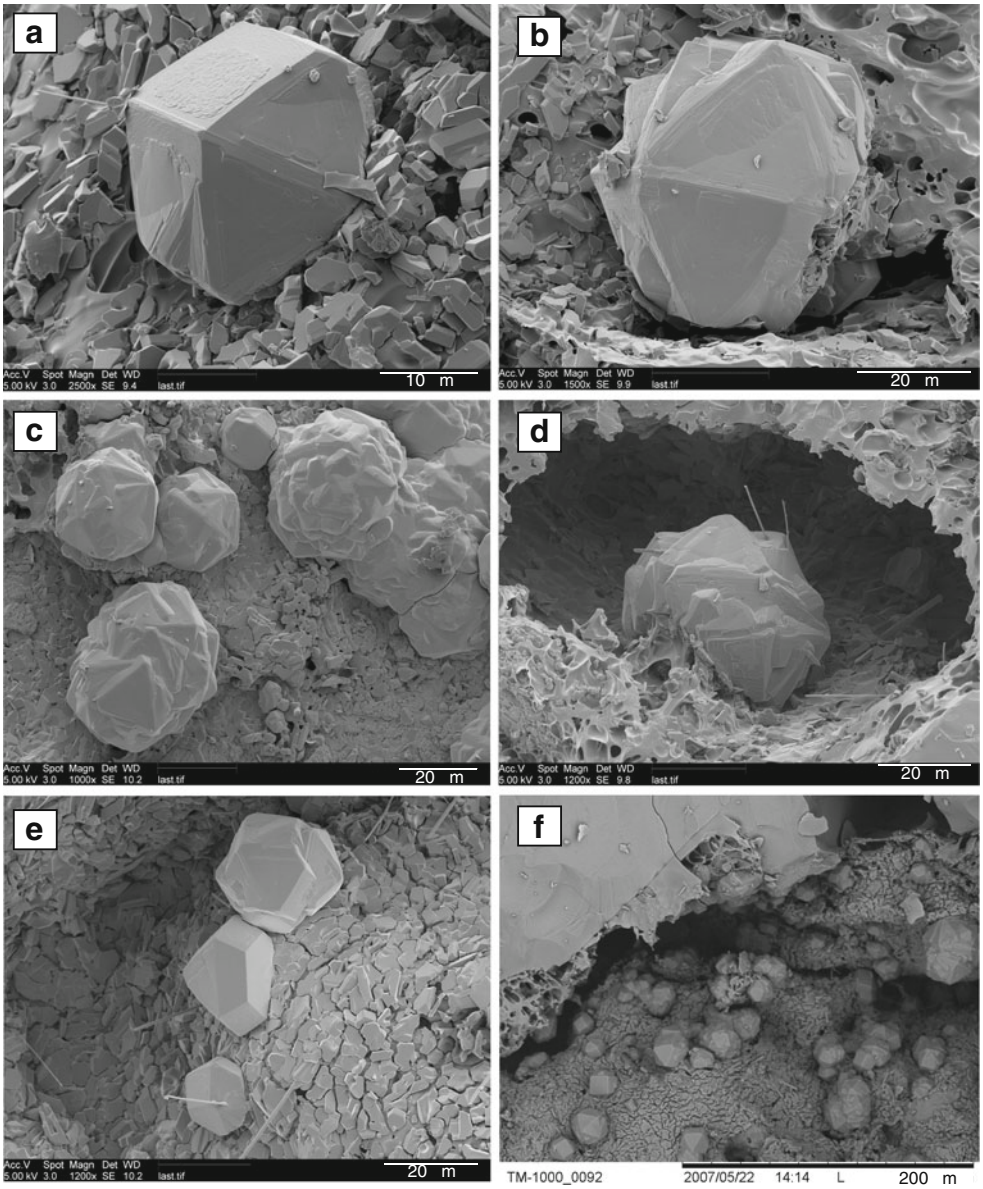

Fig. 3 SEM photomicrographs of prismatic cristobalite in rough chips of dome rock. **a**–**e** MVO287; **f** MVO819

plagioclase crystals which are often poorly formed (Fig. 1f). In addition, we noted that these samples also contained open spaces surrounding the microlites (e.g. Fig. 4b).

To put these observations into context, Table 2 summarises these crystalline forms along with others described in the literature at dome-forming volcanoes.

Other minerals

Other minerals were observed in the pore spaces including abundant plagioclase and occasional Mg-bearing phases (possibly periclase, brucite or magnesite) and TiO_2 (in MVO287, probably rutile), hornblende (in MVO1406 and MVO287) and halite (in MVO617). Sub-solidus crystallisation of plagioclase could not be identified from thin sections, but examination of rough chips by SEM clearly showed a crust of feldspar crystals lining some vugs (e.g. Fig. 3a, e and f).

Crystalline silica content of dome rocks

Cristobalite content of the dome rock samples ranges from 1.2 to 11.1 wt.%, determined using the XRD-PSD IAS method (Table 3) (with<3 % error; Le Blond et al. 2009). The lowest abundances are found in the more vesicular samples (e.g. MVO288 and MVO332). The samples with the most abundant cristobalite are dense dome rock, including the ancient sample MVO819 (174 k.a. B.P.). For most samples, quartz was not detected by XRD. However, MVO945 (400 a B.P., dense dome rock) and MVO1236 (12 July 2003, dense dome rock) both contain ~5 wt.% quartz, MontR1 (20 May 2006, dense dome rock) contains

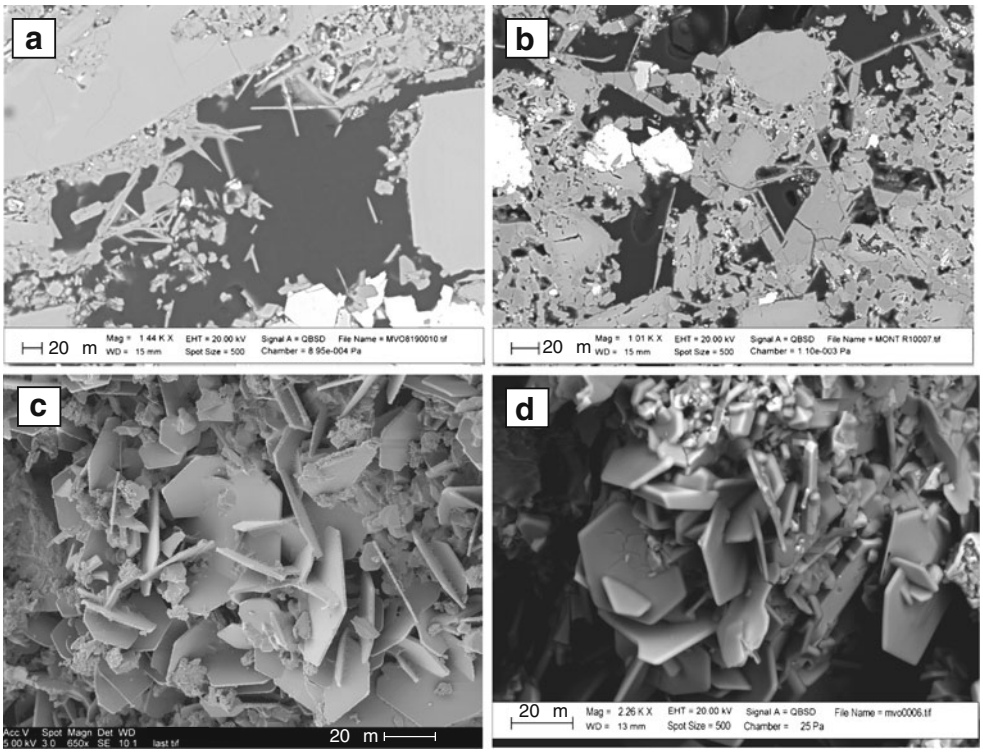

Fig. 4 Morphologies of prismatic cristobalite. **a**, **b** are backscattered electron images of MVO819 and MontR1, respectively. **c**, **d** are images of rough chips of dome rock samples MVO819 and MVO1236, respectively

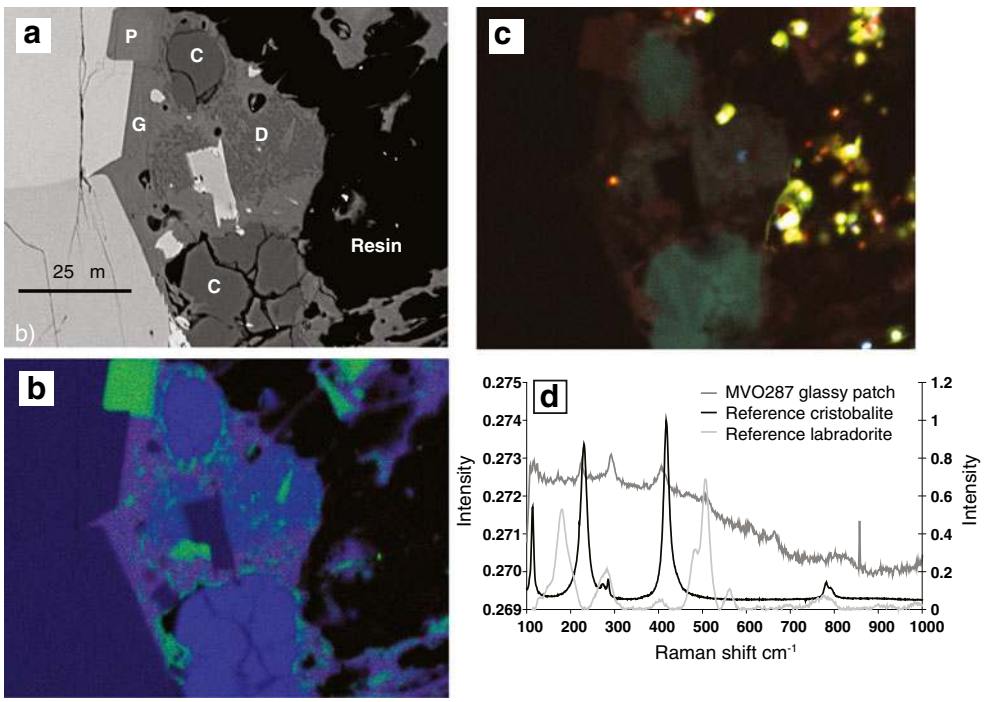

Fig. 5 **a** Backscattered electron image of sample MVO287 showing cristobalite (*C*) with fish-scale cracking and plagioclase (*P*) microlites in volcanic glass (*G*). '*D*' is a patch of devitrified glass; **b** X-ray elemental map of the same area as in (**a**) showing relative counts for Si in *blue*, Al in *green* and K in *red*, and mixtures of these colours where more than one element exists (each colour has a relative scale from black (zero counts) to the primary colour at maximum counts). Areas of volcanic glass are *purple* due to the presence of K (*red*) in addition to Si (*blue*) and Al (*green*); **c** SEM-cathodoluminescence image of the same area as in (**a**). The very *bright green/yellow areas* are artefacts from the sample preparation process; **d** Raman spectrum for a partially devitrified area of glass from MVO287 with library spectra for labradorite and cristobalite. Spike in glass spectrum at ~875 cm^{-1} is a cosmic ray artefact

Table 2 Summary of crystalline silica habits observed at dome-forming volcanoes

Silica polymorph	Morphology in thin section	Size	Interpretation	Magma type	Volcano	Key references
Quartz	Rounded and often embayed	Up to ~1 mm	Magmatic phenocryst	Andesitic–rhyolitic	Many	Murphy et al. 2000
Quartz	Subhedral, hexagonal	~10 μm	Devitrification product	Andesitic–dacitic	SHV, MSH	This study; Pallister et al. 2008
Cristobalite	Prismatic (3D), euhedral, fish-scale cracking, seen in vesicles	Up to~50 μm	Vapour-phase mineralisation	Andesitic–rhyolitic	SHV, MSH, Mt. Pelée, Inyo Domes	This study; Baxter et al. 1999; Pallister et al. 2008
Cristobalite	Platy (3D), hexagonal, acicular, fish-scale cracking, seen in vesicles	Up to ~30 μm	Vapour-phase mineralisation	Andesitic–dacitic	SHV, MSH	This study; Hoblitt and Harmon, 1993; Pallister et al. 2008 (identified as tridymite in both studies)
Cristobalite	Within groundmass with diffuse borders, fish-scale cracking	<50 μm	Devitrification product	Andesitic–dacitic	SHV	This study
Cristobalite	Feathery, inter-grown with feldspar and glass	<5 μm	Devitrification product	Andesitic–dacitic	SHV, MSH, Santiaguito	This study; Harford et al. 2003; Scott et al. 2013
Cristobalite	Lath, cutting across groundmass	Up to ~75 μm	Devitrification product?	Dacitic	MSH	Cashman et al. 2008
Cristobalite	Spherulitic, inter-grown with k-feldspar	Up to several millimetres	Devitrification product	Rhyolitic	Obsidian domes	Dadd 1992; Swanson et al. 1989
Cristobalite	Nano-fibre	<0.1 μm	Growth from vapour within eruption column	Rhyolitic	Chaitén	Reich et al. 2009
Tridymite	Arrow head with twin	Up to ~1 mm	Vapour-phase mineralisation?	Rhyolitic	Obsidian domes	Unpublished data
Tridymite	Acicular	<20 μm	Devitrification?	Dacitic	MSH	Cashman et al. 2008

Question marks in the Interpretation column indicate our interpretation of published images. Magma types are speculative. Morphologies describe thin section appearance, although 3D morphology given where observation of rock chips allowed imaging into pore spaces

Table 3 Quantification of silica phases by X-ray diffraction

Sample	Lava type	Cristobalite wt.%	Quartz wt.%	Total crystalline silica (wt.%)
MVO288	Highly vesicular	1.2	n.d.	1.2
MVO332	Vesicular	1.9	n.d.	1.9
MVO617	Dense	4.9	n.d.	4.9
MVO287	Vesicular	4.8	1.5	6.3
MVO945	Ancient, dense	2.3	4.8	7.1
MVO1406	Dense	7.8	n.d.	7.8
MVO819	Ancient, dense	8.2	n.d.	8.2
MVO1236	Dense	4.7	5.0	9.7
MontR1	Dense	11.1	2.7	13.8

All data have 1–3 wt.% error

n.d. not detected

2.7 wt.% quartz and MVO287 (21 Sept. 1997 vesicular sample) contains 1.5 wt. % quartz. These quartz quantities match the observations of devitrification-derived quartz for MVO945, MVO1236 and MontR1 (type 5, above), and we believe that MVO287 contained unusually high levels of magmatic quartz phenocrysts (observable in SEM) as there was no evidence of extensive devitrification in this sample. Tridymite was not identified in any sample.

Dome whole-rock major element compositions

XRF data are presented in Table 4 for dome rock samples (from this study and those in Devine et al. 1998; Murphy et al. 2000; Zellmer et al. 2003) and for pumice samples (analysed for this study as well as samples from Murphy et al. 2000; Zellmer et al. 2003).

The dome rock samples show a narrow range (~4 wt.%) of SiO_2 values, with the pumice data sitting amongst the dome rock data. We note that the two vesicular samples MVO288 (57.2 wt.% SiO_2) and MVO287 (61.4 wt.% SiO_2) bracket the SiO_2 range. Both samples are assumed to be from the same magma injection event (Williamson et al. 2010), but MVO287 contains some cristobalite (5.1 wt.%) and quartz (4.1 wt.%) whereas MVO288 contains rather less (1.1 wt.% cristobalite and no detectable quartz). No correlation was found between whole-rock SiO_2 content and cristobalite content (variation diagram not shown) for our dome rock samples.

Discussion

The origin of cristobalite in the Soufrière Hills domes

Two mechanisms have been proposed to explain the origin of cristobalite as a metastable mineral in lava domes:

Table 4 Whole-rock analyses by XRF for Soufrière Hills dome rocks and pumices (oxide wt.%)

Sample	Type	SiO_2	TiO_2	Al_2O_3	Fe_2O_3	MnO	MgO	CaO	Na_2O	K_2O	P_2O_5	LOI	Total
MVO288	Dome	57.20	0.69	18.41	8.27	0.18	3.15	8.41	3.20	0.63	0.14	0.18	100.45
MVO332	Dome	57.84	0.73	17.32	8.81	0.23	3.53	7.94	3.11	0.69	0.15	0.10	100.45
MVO617	Dome	58.18	0.68	18.04	7.91	0.18	3.05	8.07	3.19	0.71	0.13	0.36	100.48
MVO819	Dome	58.19	0.59	17.07	6.43	0.15	3.23	7.37	3.85	0.72	0.10	1.67	99.37
MontR1	Dome	58.63	0.69	17.19	8.24	0.20	3.40	7.83	3.17	0.75	0.14	0.10	100.35
MVO1406	Dome	59.19	0.65	17.84	7.41	0.18	3.26	8.07	3.18	0.73	0.12	-0.18	100.46
MVO945	Dome	59.42	0.67	16.95	7.87	0.20	3.03	7.42	3.23	0.76	0.14	0.69	100.38
MVO1236	Dome	60.08	0.61	18.42	6.73	0.16	2.96	7.74	3.40	0.78	0.12	0.39	101.39
MVO287	Dome	61.37	0.54	17.87	6.05	0.16	2.54	7.43	3.43	0.82	0.12	0.36	100.69
MVO289	Pumice	57.78	0.61	18.16	7.50	0.18	2.85	7.90	3.51	0.78	0.14	0.09	99.51
MVO244	Pumice	58.68	0.60	17.92	7.29	0.18	2.75	7.59	3.56	0.82	0.14	0.14	99.68
MVO291	Pumice	59.28	0.57	17.94	6.93	0.17	2.58	7.46	3.62	0.86	0.14	0.23	99.78
MVO374	Pumice	59.55	0.58	18.02	7.13	0.18	2.58	7.39	3.58	0.82	0.14	0.14	100.13
MVO1151 [c]	Dome	58.13	0.63	18.02	7.67	0.18	3.04	7.61	3.77	0.80	0.15	-0.14	100.00
MVO332 [a]	Dome	58.15	0.63	18.10	7.53	0.18	3.06	7.50	2.69	0.72	0.15	-0.13	99.57
MVO40 [c]	Dome	58.73	0.63	17.76	7.52	0.18	2.89	7.51	3.85	0.79	0.15	-	100.00
MVO201 [a]	Dome	59.08	0.62	18.09	7.30	0.18	2.89	7.56	3.45	0.75	0.15	-0.09	99.97
MVO34 [a]	Dome	59.13	0·63	18.29	7·50	0·19	2.91	7.57	3.58	0.77	0.15	-0.21	100.51
MVO231 [a]	Dome	59.15	0.63	18.01	7.35	0.18	3.05	7.64	3.66	0.72	0.14	-0.17	100.36
MVO104 [c]	Dome	59.33	0.64	17.75	7.28	0.17	2.96	7.61	3.39	0.73	0.14	-	100.00
MONT140 [b]	Dome	59.46	0.66	17.90	6.89	0.23	2.77	7.53	3.64	0.81	0.15	-	99.82
MONT128 [b]	Dome	59.72	0.58	18.26	6.61	0.13	2.80	7.43	3.33	0.92	0.14	-	99.92
MONT153 [b]	Dome	60.11	0.67	17.53	7.10	0.18	2.89	7.44	3.49	0.78	0.11	-	100.32
MVO47 [a]	Dome	60.12	0.65	17.29	7.42	0.18	2.97	7.39	3.35	0.77	0.14	-0.06	100.24
MVO1174 [c]	Dome	60.25	0.58	17.25	7.15	0.17	2.57	7.12	3.77	0.98	0.15	-0.05	100.00
MVO665L [c]	Dome	60.28	0.57	16.80	7.25	0.18	2.85	7.18	3.87	0.87	0.15	-	100.00
MVO1078 [c]	Dome	62.03	0.54	17.19	6.33	0.16	2.35	6.49	3.74	1.03	0.14	-	100.00
MVO237 [a]	Pumice	59.62	0.60	17.83	6.71	0.17	2.78	6.94	3.42	0.80	0.14	0.59	99.60
MVO244 [c]	Pumice	59.75	0.60	17.54	7.08	0.18	2.94	7.33	3.66	0.78	0.14	-	100.00

See Table 1 for sample descriptions of samples in top part of table, which were analysed for this study. The lower half of the table displays data taken from the literature (Devine et al. 1998; Murphy et al. 2000; Zellmer et al. 2003). Highlighted cells (in grey) show dome rock SiO_2 data greater than the pumice data

[a] Data from Murphy et al. 2000

[b] Data from Devine et al. 1998. For these samples, Fe is calculated as FeO, not Fe_2O_3

[c] Data from Zellmer et al. 2003. Only samples clearly identifiable as dome rock/pumice from the MVO sample database were used

vapour-phase transport and deposition, and devitrification of groundmass glass (e.g. Baxter et al. 1999). Through careful observations of crystalline silica textures in Soufrière Hills dome rock, this study affirms that both were likely emplacement mechanisms in Soufrière Hills dome lava.

Vapour-phase mineralisation

Prismatic cristobalite was found throughout the dome rock samples analysed in this study, from occasional crystals within vesicles in pumiceous samples to filling most pore spaces in dense dome rock. The prismatic cristobalite appears to be a ubiquitous feature of the Soufrière Hills dome lava.

The morphology of cristobalite varies from well-formed single, prismatic crystals, to forms with multiple, interlocking twins and, in some cases, platy, hexagonal crystals. The causes of these morphological variations are unclear, possibly relating to differences in vapour fluxes and composition, and fluctuations in temperature and pressure. Horwell et al. (2012) have shown that prismatic and platy cristobalite at SHV contain structural substitutions of aluminium and sodium (up to 3 wt.% Al_2O_3 and 1 wt.% Na_2O) with platy cristobalite containing significantly more substituted cations than prismatic cristobalite so morphology may be influenced by structural variations.

Prismatic cristobalite crystals are often observed growing into open pore spaces and fractures within the dome rock (Fig. 1c) leading us to interpret that these crystals have precipitated from vapour-phase fluids passing through the permeable dome. We also observe this form of cristobalite as patches in dense dome rock and conclude that, in instances where the boundaries of the crystal can be clearly identified, cristobalite has been deposited from a vapour

phase and has almost completely filled the available pore space (Fig. 1d). In some circumstances, it is difficult to determine a clear boundary between the cristobalite patches and the groundmass (Fig. 1c and e); in this case, the cristobalite may be the product of extensive devitrification, or of vapour-phase deposition on devitrification cristobalite. We also interpret the platy crystals as being vapour-phase precipitates.

Devitrification

We interpret the areas of 'feathery' groundmass containing micro-crystals of cristobalite to be formed by devitrification of the SHV glass (e.g. Fig. 1e) and the glass-free, quartz/cristobalite/feldspar microlite-rich areas as being patches of total devitrification. Little work has been done on devitrification of andesitic/dacitic dome rocks. However, Blundy and Cashman (2001), Cashman (1992), Harford et al. (2003) and Couch et al. (2003a) all recognised two types of glass at MSH and SHV: a 'true' glass and a glass with "very finely crystalline intergrowths of feldspar and quartz" (Couch et al. 2003a), which we believe to be devitrification patches similar (MSH) or identical (SHV) to those observed in this study (through comparison of their images with our textural observations). Production of spherulites by devitrification of rhyolitic obsidian is common (e.g. Swanson et al. 1989), but we did not observe spherulites in the andesitic SHV lavas, and, unlike in spherulites, the devitrification phases observed here were not in the form of axiolitic, radiative or acicular intergrowths. We have also clarified that the crystalline silica phase in devitrification glass at SHV is cristobalite unless complete devitrification occurs in which case thermodynamic factors may allow conversion of metastable cristobalite to quartz.

Harford et al. (2003) show that patches of devitrified glass at SHV are chemically distinct from true glass: K_2O (4–6 wt.% in true glass) is depleted in the devitrified glass (0.5 wt.%); Na_2O is slightly enriched (3.9 wt.% compared with 2.4–3.3 wt.% for true glass); and devitrified glass does not contain chlorine. The depletion of K and the absence of Cl indicates that volatiles are lost during devitrification; we conclude that these volatiles are likely transported to surface fumaroles in passing vapours, as we do not observe any K or Cl-bearing minerals (except rare halite in one sample) as vapour-phase precipitates within the dome. As far as we can tell, no studies have been carried out on active, magmatic-water-dominated fumaroles on Montserrat—those studied by Boudon et al. (1998) were venting fluids of mainly sea-water origin—and therefore, the precipitation of K-bearing phases cannot be assessed.

All samples containing vapour-phase cristobalite also showed devitrification textures, except the pumiceous sample MVO288 which only had trace amounts of vapour-phase cristobalite (by SEM). This supports the theory of Jones and Segnit (1972) which implies that vapour-phase cristobalite precipitation requires the pre-existence of devitrification cristobalite for nucleation (see "Cristobalite formation mechanisms"). It is possible that MVO288 contained devitrification cristobalite nuclei beyond the resolution of the SEM.

Scott et al. (2013) and Horwell et al. (2013) propose that the extent of devitrification in dome rock is related to the rate of lava extrusion, with slow extrusion promoting greater devitrification as the lava is held at suitable pressure/temperature conditions for longer.

Local redistribution versus bulk transport

The collection of XRD and XRF data for cristobalite and SiO_2 contents in the various Soufrière Hills dome rocks has allowed us to investigate the mechanisms of silica transport for vapour-phase mineralisation. Understanding the mechanisms and rate of formation of cristobalite is important because it affects the distribution and abundance of silica within the conduit/dome system. The formation of vapour-phase cristobalite in dome rock requires the transport of silica, via local redistribution (over the length-scale of individual crystals and vugs), via bulk transport from one part of the magmatic/hydrothermal system to another or, perhaps, via both routes.

Local redistribution of silica may result when reactive species, such as Cl and F, are trapped in closed vugs, where they may corrode amorphous glass and precipitate crystalline silica (e.g. via the reaction in Eq. 1). In experiments by Hammer and Rutherford (2002), vapour-phase cristobalite was grown (fish-scale prismatic crystals observed within vesicles, labelled as quartz) during decompression of Pinatubo dacitic pumice, providing evidence that, in experimental settings at least, cristobalite can form without an external vapour source (i.e. local redistribution).

Bulk transport may result from the flow of silica-bearing gases from parts of the magmatic system where pressure, temperature and speciation favour silica corrosion, to parts of the system where conditions favour mineralisation. If we consider the pressure and temperature dependence of the equilibrium of Eq. 1, we can infer from de Hoog et al. (2005) that higher pressures in the conduit favour silica corrosion and lower pressures in the dome favour mineralisation.

Bulk transport of silica would be expected to lead to changes in the bulk (whole rock) SiO_2 content of dome rock over time, whilst local redistribution would not (we note that, since devitrification involves redistribution of silica over very short distances only, it will not, on its own, cause a change in the bulk SiO_2 content of a packet of dome rock). In order to assess whether bulk transport has affected SiO_2 content in SHV dome rock, we compared the whole-rock compositions of samples of dome rock (from this study and Devine et al. 1998; Murphy et al. 2000; Zellmer et al. 2003) and explosive pumice (from this study and Murphy et al. 2000; Zellmer et al. 2003). Whilst pumice compositions should reflect the original

magmatic assemblage, since cristobalite does not form during the magmatic phase, the composition of dome rock samples may have been altered by the addition of SiO_2. The data (Table 4) demonstrate that the SiO_2 content of SHV dome rock samples fall in the range 57.2–62.0 wt.%, and pumice samples fall in the range 57.8–59.8 wt.%; the seven samples with the highest SiO_2 content are all dome rocks (highlighted in Table 4). Whilst this is not conclusive, it suggests that some dome rock samples have been enriched in SiO_2, relative to magmatic compositions, consistent with the hypothesis of bulk transport. For our samples, however, we also compared cristobalite content with bulk SiO_2 content, to see if samples with high cristobalite also had enriched SiO_2, but found no relationship between the two.

To aid with the interpretation of these results, it is useful to consider two contrasting scenarios. (1) If we assume that there is no bulk transport of silica, then the measured SiO_2 content of the samples must reflect the initial composition of the parent magma. In this scenario, the observed variation in SiO_2 content would indicate that the composition of the parent magma varied over a 5 wt.% interval over time and space (between ~57 and 62 wt.%), which is not uncommon in intermediate lavas and may also be the product of local heterogeneity in crystal assemblages. (2) If, instead, we assume that the composition of the parent magma is fixed, then any variations in measured SiO_2 content should reflect the bulk transport of SiO_2. To illustrate this effect, consider the vapour-phase mineralisation of a 100 g sample of dome rock sample MVO288 (vesicular sample containing only trace amounts of cristobalite). This sample has an initial SiO_2 content of 57 wt.% (Table 4; i.e. 57 g of the sample is SiO_2); if bulk transport of SiO_2 adds 10 wt.% cristobalite to the sample, the mass of the sample is now 111 g (of which 11.1 g is cristobalite). If the cristobalite is 98 wt.% SiO_2 (consistent with the range observed by Horwell et al. 2012), this mineralisation adds 10.9 g of SiO_2 to the sample so that 67.9 g of the 111 g sample is now SiO_2. The bulk SiO_2 content of the mineralised sample is, therefore, 61.1 wt.%; i.e. addition of 10 wt.% cristobalite increases the bulk SiO_2 content by only 4.1 wt.%. In general, the change in wt.% SiO_2 (ΔSiO_2) due to the addition of wt.% of a mineral W_{min} is given by:

$$(\Delta SiO_2) = \frac{W_{min}(X_{min} - X_0)}{100} \quad (2)$$

where X_{min} is the SiO_2 content of the added mineral in weight percent and X_0 is the initial SiO_2 content of the sample in weight percent. From this equation, we can see that the modest variation in bulk SiO_2 content that we measure in our samples (5 wt.%) is consistent with the addition of up to 12 wt.% vapour-phase cristobalite through bulk transport. Note that the addition of vapour-phase plagioclase has a much smaller impact on bulk SiO_2 content because X_{min} (~53 wt.% for labradorite; Deer et al. 1996) is very similar to X_0.

The compositional data alone do not allow us to determine conclusively whether the observed variation in silica content results from bulk transport of SiO_2, from variation in SiO_2 composition of the parent magma, or some combination of the two. However, we note that our textural observation that cristobalite almost completely in-fills relict porosity in some samples (e.g. MVO1406; dense dome lava from 20 May 2006 collapse) favours the bulk transport of SiO_2. The bulk transport of even modest amounts of SiO_2, therefore, could have important consequences for the interpretation of petrological and geochemical studies, and for porosity/permeability relationships which will affect the evolution of the stability of the dome; these consequences are considered in sections "Implications for petrological and geochemical studies" and "Implications for the evolution of lava dome stability" below.

Timescale of cristobalite formation and evolution

From studies of a single pyroclast from Montserrat (MVO287), believed to represent magma injected into the dome during the switch from effusive to explosive activity, cristobalite crystallisation appears to have occurred while the magma was still plastic (Williamson et al. 2010), probably within hours or days of the magma entering the upper conduit or dome environment. The short residence time of this material in the dome indicates that cristobalite crystallisation can be extremely rapid as the sample has 4.8 wt.% cristobalite and has both vapour phase and devitrification textures. This conclusion is supported by Horwell et al. (2010), who found 16 wt.% cristobalite in ash from the August 2008 collapse of the Chaitén (Chile) lava dome, just 3 months after the onset of dome growth (N.B. quantities of cristobalite are likely to be somewhat concentrated in co-ignimbrite ashfall compared with dome rock (Horwell et al. 2001)). Sample MVO288 was collected from the same deposit as MVO287 and is believed to have been part of the same magma injection event but was perhaps located slightly deeper in the dome at the time of collapse (Williamson et al. 2010). MVO288 contains just a few vapour-phase cristobalite crystals and no devitrification textures (see "Discussion," above). The difference in residence time in the dome of these two samples may be as little as a few hours.

Ostwald's rule of stages states that the first phase to crystallise from a melt is often the thermodynamically unstable polymorph, which then re-crystallises to form the thermodynamically stable phases (Nývlt 1995). This appears to be the case with cristobalite in volcanic domes, but the kinetics also seem such that re-crystallisation to quartz does not occur except during extensive devitrification. Analysis of our oldest sample (MVO819) indicates that, even over timescales of hundreds of thousands of

years, vapour-phase cristobalite does not transform to quartz, perhaps because there is insufficient energy for the reconstructive transformation (involving bond breakage) (Deer et al. 1996).

Duffy (1993) calculates that the conversion time for cristobalite to quartz at 35 °C (and at atmospheric pressure) is less than 10^5 years; however, experimental studies by Ernst and Calvert (1969) determined conversion times of tens of millions of years. This reconstructive transformation will hence be very slow, or will not occur if there is insufficient energy to break and re-form the bonds in the silica structure. The presence of quartz in totally devitrified samples (such as MVO1236) indicates that, in some environments, cristobalite formed by devitrification of glass can undergo reconstructive transformations to quartz very rapidly (collected from a total dome collapse on 12 July 2003, this sample was derived from dome material <24 months old; Horwell et al. 2013). We infer this from textures which indicate that the sub-hedral quartz was once part of a larger fish-scale crystal (Fig. 1f), although there is evidence in the experimental literature of quartz forming directly by devitrification (Lofgren 1971). The transformation could be initiated by heating and throughput of volatiles related to the new injection of magma into the dome. Alternatively, re-crystallisation might be caused by the circulation of hydrothermal fluids.

Further implications

Mineralisation of the dome through bulk transport of SiO_2-bearing vapours has important implications for the evolution of the physical properties of the dome, and for the interpretation of geochemical and petrological investigations of dome rock. Whilst our XRF data do not conclusively demonstrate that bulk transport has occurred at SHV, the textural evidence is sufficiently compelling to warrant consideration of its consequences. In particular, we observe that vapour-phase cristobalite (and subordinate vapour-phase plagioclase) partially fills pore space in all dome samples; furthermore, in some dense dome rock samples (notably MVO1406), pore space is almost completely occluded by vapour-phase mineralisation, indicating that the samples have undergone dramatic textural changes.

Implications for petrological and geochemical studies

The bulk transport of silica, in the vapour phase, from one part of the conduit/dome system to another may progressively change the composition and mineralogy of the dome rock. Consequently, samples of dome rock may not be strictly representative of the initial magma from which they are derived, as assessed in "Local redistribution versus bulk transport". If this is not taken into consideration in the petrological and geochemical analysis of dome rocks, it could lead to incorrect interpretations and poorly posed experimental studies.

Cristobalite has previously been identified in thin sections of dome rock from several volcanoes, including Mt. Pelée, Martinique (Martel et al. 2000) and MSH (e.g. Pallister et al. 2008 Fig. 10b and c). However, we believe that it has also been misidentified or misnamed in the literature as quartz (perhaps as a generic name for crystalline, or crypto-crystalline silica) at SHV (e.g. Couch et al. 2003b) and as quartz or tridymite at MSH (e.g. Hoblitt and Harmon 1993; Blundy and Cashman 2001; Pallister et al. 2008), based on SEM images showing the signature fish-scale cracking in those articles. Images of SHV samples MVO1217 and MVO34 (Fig. 16, Couch et al. 2003b) show them to be rich in vapour-phase, fish-scale cristobalite (labelled as 'quartz'). It has also been misidentified as quartz in experimental crystallisation studies (e.g. Hammer and Rutherford 2002; Couch et al. 2003a; Couch et al. 2003b) where fish-scale cristobalite has grown in preference to quartz.

Misidentification of vapour-phase cristobalite as primary quartz is important in experimental studies because whole-rock compositions are commonly used for partial or total phase equilibrium studies to determine pre-eruptive parameters such as P, T, fH_2O and fO_2 in magmatic systems. These fundamental parameters underpin a variety of further activities, for example, petrological monitoring of active volcanoes, determining magmatic timescales, depths of magma storage, pre-eruptive volatile composition of the magma and the composition of magmatic gases (Pichavant et al. 2007). Consequently, it is critical that they are constrained as accurately as possible. Experiments are typically conducted using material thought to have the same composition as the magma of interest, based on the whole rock composition of lava.

Pichavant et al. (2007) recognised that, sometimes, experiments are unable to reproduce phenocryst assemblages, indicating a compositional mismatch between the experimental material and the reactive magma (e.g. Holtz et al. 2005). We propose that such a mismatch could result if lava samples are affected by bulk transport. For example, Barclay et al. (1998) used a crushed and melted Soufrière Hills dome sample (MVO34, erupted in Feb. 1996, the same sample as used by Couch et al. 2003b, see above) for melting and crystallisation experiments to constrain the pressure, temperature and $X(H_2O)$ of the magma storage conditions prior to ascent and eruption. As described above, it appears from Fig. 16 in Couch et al. (2003b) that this sample contains vapour-phase cristobalite. It is possible that elevated levels of SiO_2 in the sample could have affected the accuracy of experiments and calculations; this could be

particularly important for the quartz stability field, which was determined to be quite narrow (<840 °C with a PH_2O of 115–130 MPa). If cristobalite in these examples is the product of bulk transport of silica from elsewhere in the magmatic system, then it represents excess silica above the magmatic composition.

Couch et al. (2003a) used the groundmass composition of MVO34 as the starting composition for crystallisation experiments to demonstrate late-stage microlite growth as a result of degassing during magma ascent. They determined the phase equilibria using the Qz-Ab-Or ternary system (after Blundy and Cashman 2001). In their Qz-Ab-Or ternary diagram, Couch et al. (2003a) found that the normative compositions of several experimental glasses (with a crystalline silica phase present) did not plot at the expected cotectic pressures. It is possible that this is because of excess silica present in the system but could also be explained by cristobalite forming metastably at lower PH_2O than expected for quartz (samples which should have plotted at 100, 50 and 25 MPa all plotted at ≤25 MPa).

It is difficult to confirm the influence of cristobalite without investigating the original samples, but the results of this study are sufficient to highlight the need for workers to select samples for experimental studies carefully to ensure that their data are not affected by the presence of secondary mineralisation.

Implications for the evolution of lava dome stability

Sample MVO1406 represents recent dense dome rock that has undergone almost complete porosity occlusion by vapour-phase mineralisation (Fig. 1d). Porosity occlusion must result in large-scale reorganisation of the gas-flow pathways through the dome, perhaps favouring flow along cracks, as permeable networks of vesicles become occluded (Fig. 6). The deposition of vapour-phase minerals within a lava dome will, therefore, affect its porosity and permeability, with important implications for dome stability. We propose two competing processes: (1) the occlusion of pore networks by vapour-phase minerals will decrease dome permeability, causing gas pressure to increase, promoting dome failure; (2) the precipitation of minerals in pore-spaces and cracks in dome rock will increase its mechanical strength making it less likely to collapse. We propose that (in addition to the other processes described in the "Introduction") dome stability is influenced by the competition between these two effects and that the evolution of dome stability over time may be influenced by progressive mineralisation (Fig. 6).

Permeability

The permeability k of dome rock depends strongly on its interconnected porosity ϕ (equivalently, its vesicularity).

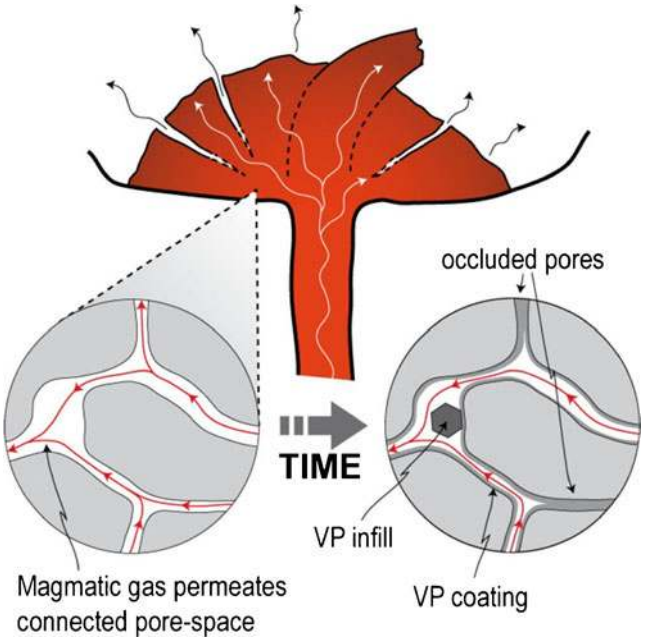

Fig. 6 Section through a dome. Over time, vapour-phase minerals precipitate from permeating gases, occluding pores and densifying rock

Mueller et al. (2005) present an empirical relationship for $k(\phi)$, based on laboratory measurements of the permeability of dome rock samples from Unzen (Japan), Merapi (Indonesia) and Shiveluch (Russia):

$$k = 10^{-17} \times \phi^{3.4}. \quad (3)$$

They find that this relationship, which is based on the Kozeny–Carman equation, is appropriate for dome rocks with porosity ϕ<0.3, where gas flows along tortuous pathways. We can use this relationship to explore the impact of vapour-phase mineralisation on the permeability of dome rock, using sample MVO287 as an example.

MVO287 has a porosity $\phi \approx 0.2$ (Williamson et al. 2010) and contains approximately 5 wt.% cristobalite. If we consider one extreme, that all of the cristobalite present in the sample was deposited from the vapour phase, into pore space, then we can calculate the original porosity of the sample before vapour-phase mineralisation:

$$\phi_0 = \frac{\phi+\alpha}{1+\alpha}, \quad where \quad \alpha = \frac{W_c}{(100-W_c)} \frac{\rho_A}{\rho_c} \quad (4)$$

where W_c is the wt.% cristobalite in the sample, ρ_A is the density of vesicle-free andesite and ρ_c is the density of cristobalite. Using ρ_A=2,600 kgm^{-3} (McBirney 1993), ρ_c=2,330 kgm^{-3} (Deer et al. 1996), and the values for ϕ and W_c given above, we find that ϕ_0=0.24, i.e. that the deposition of vapour-phase cristobalite has caused the porosity to decrease from 0.24 to 0.20. From Eq. 3, this corresponds to a decrease in permeability of a factor of 2 (from 5.2×10^{-13} to 2.7×10^{-13}m^2).

The calculation above, whilst illustrative, rather than definitive, does indicate that occlusion of porosity by vapour-phase mineralisation has had an important effect on the permeability of sample MVO287, and it should be noted that this sample was unusually vesicular for dome rock. More generally, the impact of mineralisation on permeability will be more pronounced for samples with a lower initial porosity, and with a greater degree of mineralisation. For example, if 10 wt.% vapour-phase cristobalite is deposited within the connected porosity of a sample with an initial porosity of ϕ_0=0.2, the final porosity is ϕ=0.1, and the permeability drops by a factor of 10, from 2.6×10^{-13} to 2.7×10^{-14} m^2. In some samples, such as MVO1406, where vapour-phase mineralisation appears to have completely filled all pore space, both the porosity and permeability will be negligible.

Rock strength

The strength of dome rock as a function of porosity has been investigated in uniaxial/triaxial compression experiments (Kennedy et al. 2009; Smith et al. 2011), in fracture toughness experiments (Scheu et al. 2008) and in decompression–fragmentation experiments (Spieler et al. 2004; Scheu et al. 2008). In all cases, the strength of dome rock is found to increase strongly as porosity decreases. None of these studies explicitly considers whether secondary mineralisation plays a role in decreasing rock porosity and increasing rock strength; however, it is known, from our own unpublished work and that of Pallister et al. (2008), that vapour-phase cristobalite is present in Mt. St. Helens 2004–2008 dome rock (used in the studies of Kennedy et al. 2009 and Smith et al. 2011) and in Unzen 1990–1995 dome rock (used in the study of Scheu et al. 2008).

Furthermore, a consideration of the microstructural controls on the failure of porous rocks suggests that progressive vapour-phase mineralisation would tend to increase rock strength. Paterson and Wong (2005) identify two different failure mechanisms for porous rocks depending on whether the solid matrix surrounding the pores is strong and coherent ('strongly cohesive'), or contains many planes of weakness ('weakly cohesive'). In strongly cohesive rocks, the pores act to localise stress, leading to micro-cracking of the pore walls; in this case, we propose that vapour-phase mineralisation will act to reinforce the pore walls and inhibit microcrack formation, hence strengthening the rock. In weakly cohesive rocks containing many pre-existing fractures, we propose that mineralisation will act to seal these fractures, again, strengthening the rock. The relationship between microstructure and rock mechanics is complex, and further work is needed to test this hypothesis; however, it seems intuitive that replacing gas-filled void spaces in a rock with crystalline material should have a significant impact on its rock mechanical properties and, hence, on the response of the dome to stress.

The calculations and experimental results discussed above indicate that occlusion of porosity by vapour-phase mineralisation—even through the addition of just 5–10 wt. % cristobalite—must substantially decrease permeability and may substantially impact the mechanical strength of dome rock. These two processes are likely to have opposing effects on dome stability: Permeability reduction will promote the development of gas overpressure within the dome, encouraging failure (Voight and Elsworth 2000); whilst an increase in mechanical strength of the rock would stabilise the dome. Dedicated work is needed to determine how these two processes interact to determine the evolution of stability of lava domes undergoing vapour-phase mineralisation.

Conclusions

Detailed observations and analysis have confirmed that cristobalite is formed both by vapour-phase mineralisation and by devitrification of volcanic glass and is ubiquitous within the Soufrière Hills dome rock. The vapour-phase cristobalite exists as prismatic and platy crystals within pore spaces whereas the devitrification cristobalite exists as feathery crystallites in the groundmass. In some dense dome rock, cristobalite almost completely fills porosity, occluding pore spaces. In some samples, glass devitrification is complete, resulting in a 'matrix' of quartz, cristobalite and feldspar with minor glass.

The rate and degree of cristobalite mineralisation is unlikely to be constant, varying with time, with position within the dome and with other factors such as magmatic activity and fluid availability. Investigation of the effects of pressure, temperature and dome residence time were not possible within the current investigation due to samples being sourced from PDC deposits rather than collected in situ from lobes. A recent analysis of SHV volcanic ash showed no correlation between dome residence time and cristobalite content except when lava extrusion rates were exceptionally high, where a positive correlation was observed (Horwell et al. 2013).

The origin of the silica that produces the vapour-phase cristobalite has important implications for the interpretation of the effects of mineralisation on whole rock compositions of domes, and on dome stability. Although we cannot categorically distinguish between bulk transport and local redistribution of silica, it is clear that a modest input of silica into the dome system can result in changes in whole rock geochemistry of several wt.% SiO_2. This has implications for the use of cristobalite-bearing samples in experimental phase-equilibrium petrological studies. The occlusion of porosity in dome rock may also have implications for dome-collapse hazard at silicic volcanoes; the addition of

just 5–10 wt.% cristobalite will impact the permeability and rock mechanical behaviour of dome rock, potentially influencing dome strength and gas pressurisation.

The observations in this study indicate that new experimental studies on the high-temperature kinetics of cristobalite formation in closed and open systems, thermodynamic modelling of cristobalite precipitation in lava domes and rock strength measurements are required to underpin more accurate assessment of the stability of lava domes.

Acknowledgements The work of CJH was supported by a Natural Environment Research Council (NERC) Postdoctoral Research Fellowship (Grant No. NE/C518081/2). JSL acknowledges a NERC CASE Studentship (NER/S/A/2006/14107) whilst at the University of Cambridge, UK. DED acknowledges a Moyes Foundation studentship. We are grateful to Sue Loughlin and Thomas Christopher from the British Geological Survey and Montserrat Volcano Observatory for access to MVO collections and guidance in the field, and to Prof. Steve Sparks (University of Bristol, UK) for providing the pumice samples. We would also like to particularly thank MVO staff for their help sourcing samples from their archives. We thank Alan Brooker of Renishaw plc for invaluable help with SEM-Raman analyses. Thanks also to NHM staff: Gordon Cressey, for advice on XRD, and Dave Smith for sample curation. Many thanks to Madeleine Humphreys (Oxford University, UK) and Yan Lavallée (University of Liverpool, UK) for useful comments on the draft manuscript and to Eliza Calder (University of Buffalo, USA) and Jenni Barclay (University of East Anglia, UK) for their helpful reviews.

References

Allen AG, Baxter PJ, Ottley CJ (2000) Gas and particle emissions from Soufriere Hills volcano, Montserrat, West Indies: characterization and health hazard assessment. Bull Volcanol 62:8–19

Barclay J, Rutherford MJ, Carroll MR, Murphy MD, Devine JD, Gardner J, Sparks RSJ (1998) Experimental phase equilibria constraints on pre-eruptive storage conditions of the Soufriere Hills magma. Geophys Res Lett 25(18):3437–3440

Baxter PJ, Bonadonna C, Dupree R, Hards VL, Kohn SC, Murphy MD, Nichols A, Nicholson RA, Norton G, Searl A, Sparks RSJ, Vickers BP (1999) Cristobalite in volcanic ash of the Soufriere Hills Volcano, Montserrat, British West Indies. Science 283:1142–1145

Baxter PJ, Searl A, Cowie HA, Jarvis D, Horwell CJ (Accepted) Evaluating the respiratory health risks of volcanic ash at the eruption of the Soufrière Hills Volcano, Montserrat, 1995–2010. In: Wadge G, Robertson R, Voight B (eds) The eruption of Soufriere Hills volcano, Montserrat from 2000 to 2010. Geol Soc Lon Mem

Blundy J, Cashman K (2001) Ascent-driven crystallisation of dacite magmas at Mount St Helens, 1980–1986. Contrib Mineral Petrol 140:631–650

Boggs SJ, Kwon Y-I, Goles GG, Rusk BG, Krinsley D, Seyedolali A (2002) Is quartz cathodoluminescence color a reliable provenance tool? A quantitative examination. J Sediment Res 72:408–415

Boudon G, Villemant B, Komorowski J-C, Ildefonse P, Semet MP (1998) The hydrothermal system at Soufriere Hills Volcano, Montserrat (West Indies): characterisation and role in the ongoing eruption. Geophys Res Lett 25:3693–3696

Calder ES, Luckett R, Sparks RSJ, Voight B (2002) Mechanisms of lava dome instability and generation of rockfalls and pyroclastic flows at Soufrière Hills Volcano, Montserrat. In: Druitt TH, Kokelaar BP (eds) The eruption of Soufrière Hills volcano, Montserrat, from 1995 to 1999. Geol Soc Lon Mem 21:173–190

Carpenter MA, Salje EKH, Graeme-Barber A (1998) Spontaneous strain as a determinant of thermodynamic properties for phase transitions in minerals. Eur J Mineral 10:621–691

Cashman KV (1992) Groundmass crystallization of Mount St Helens dacite, 1980–1986—a tool for interpreting shallow magmatic processes. Contrib Mineral Petrol 109:431–499

Cashman KV, Thornber CR, Pallister JS (2008) From dome to dust: shallow crystallization and fragmentation of conduit magma during the 2004–2006 dome extrusion of Mount St. Helens, Washington. In: Sherrod DR, Scott WE, Stauffer PH (eds) A volcano rekindled: The renewed eruption of Mount St. Helens, 2004–2006. U.S. Geological Survey Professional Paper, pp 387–413

Churakov SV, Tkachenko SI, Korzhinskii MA, Bocharnikov RE, Shmulovich KI (2000) Evolution of composition of high-temperature fumarolic gases from Kudryavy Volcano, Iturup, Kuril Islands: the thermodynamic modeling. Geochem Int 38 (5):436–451

Couch S, Harford CL, Sparks RSJ, Carroll MR (2003a) Experimental constraints on the conditions of formation of highly calcic plagioclase microlites at the Soufriere Hills volcano, Montserrat. J Petrol 44(8):1455–1475

Couch S, Sparks RSJ, Carroll MR (2003b) The kinetics of degassing-induced crystallization at Soufriere Hills volcano, Montserrat. J Petrol 44(8):1477–1502

Dadd KA (1992) Structures within large volume rhyolite lava flows of the Devonian Comerong Volcanics, southeastern Australia, and the Pleistocene Ngongotaha lava dome, New Zealand. J Volcanol Geotherm Res 54(1–2):33–51

Damby DE, Horwell CJ, Baxter PJ, Delmelle P, Donaldson K, Dunster C, Fubini B, Murphy F, Nattrass C, Sweeney S, Tetley T, Tomatis M (2013) The respiratory health hazard of tephra from the 2010 Centennial eruption of Merapi with implications for occupational mining of deposits. J Volcanol Geotherm Res. doi:10.1016/j.jvolgeores.2012.09.001

de Hoog JCM, van Bergen MJ, Jacobs MHG (2005) Vapour-phase crystallisation of silica from SiF_4-bearing volcanic gases. Ann Geophys 48(4/5):775–785

Deer WA, Howie RA, Zussman J (1996) An introduction to the rock forming minerals. Longman Scientific and Technical, New York, p 696

Devine JD, Murphy MD, Rutherford MJ, Barclay J, Sparks RSJ, Carroll MR, Young SR, Gardner JE (1998) Petrologic evidence for pre-eruptive pressure-temperature conditions, and recent reheating, of andesitic magma erupting at the Soufriere Hills Volcano, Montserrat, WI. Geophys Res Lett 25:3669–3672

Druitt TH, Young SR, Baptie BJ, Bonadonna C, Calder ES, Clarke AB, Cole PD, Harford CL, Herd RA, Luckett R, Ryan G, Voight B (2002) Episodes of cyclic vulcanian explosive activity with fountain collapse at Soufrière Hills Volcano, Montserrat. In: Druitt TH, Kokelaar, B P, (ed) The eruption of Soufrière Hills volcano, Montserrat, from 1995 to 1999. Geol Soc Lon Mem 21:281–306

Duffy CJ (1993) Kinetics of silica-phase transitions. In: Los Alamos National Lab., NM (United States), Report number LA-12564-MS, p 22

Edmonds M, Oppenheimer C, Pyle DM, Herd RA, Thompson G (2003) SO_2 emissions from Soufriere Hills volcano and their relationship to conduit permeability, hydrothermal interaction and degassing regime. J Volcanol Geotherm Res 124(1–2):23–43

Elsworth D, Voight B (2001) The mechanics of harmonic gas pressurization and failure of lava domes. Geophys J Int 145:187–198

Elsworth D, Voight B, Thompson G, Young SR (2004) Thermal-hydrologic mechanism for rainfall-triggered collapse of lava domes. Geology 32:969–972

Ernst WG, Calvert SE (1969) An experimental study of the recrystallization of porcelanite and its bearing on the origin of some bedded cherts. Am J Sci 267-A:114–133

Foustoukos DI, Seyfried WEJ (2007) Quartz solubility in the two-phase and critical region of the NaCl–KCl–H_2O system: implications for submarine hydrothermal vent systems at 9°50'N East Pacific Rise. Geochim Cosmochim Acta 71:186–201

Getahun A, Reed MH, Symonds R (1996) Mount St. Augustine volcano fumarole wall rock alteration: mineralogy, zoning, composition and numerical models of its formation process. J Volcanol Geotherm Res 71(2–4):73–107

Hammer J, Rutherford M (2002) An experimental study of the kinetics of decompression-induced crystallization in silicic melt. J Geophys Res 107(B1):2021

Harford CL, Pringle MS, Sparks RSJ, Young SR (2002) The volcanic evolution of Montserrat using $^{40}Ar/^{39}Ar$ geochronology. In: Druitt TH, Kokelaar BP (eds) The eruption of Soufrière Hills Volcano, Montserrat, from 1995 to 1999. Geol Soc Lon Mem 21:93–113

Harford CL, Sparks RSJ, Fallick AE (2003) Degassing at the Soufriere HIlls volcano, Montserrat, recorded in matrix glass compositions. J Petrol 44(8):1503–1523

Hicks PD, Matthews AJ, Cooker MJ (2009) Thermal structure of a gas-permeable lava dome and timescale separation in its response to perturbation. J Geophys Res 114:B07201

Hoblitt RP, Harmon RS (1993) Bimodal density distribution of cryptodome dacite from the 1980 eruption of Mount St. Helens, Washington. Bull Volcanol 55:421–437

Holtz F, Sato H, Lewis J, Behrens H, Nakada S (2005) Experimental petrology of the 1991–1995 Unzen dacite, Japan. Part I: phase relations, phase compositions and pre-eruptive conditions. J Petrol 46:319–337

Horwell CJ, Baxter PJ (2006) The respiratory health hazards of volcanic ash: a review for volcanic risk mitigation. Bull Volcanol 69 (1):1–24

Horwell CJ, Braña LP, Sparks RSJ, Murphy MD, Hards VL (2001) A geochemical investigation of fragmentation and physical fractionation in pyroclastic flows from the Soufriere Hills volcano, Montserrat. J Volcanol Geotherm Res 109(4):247–262

Horwell CJ, Hillman SE, Cole PD, Loughlin SC, Llewellin EW, Damby DE, Christopher T (2013) Controls on variations in cristobalite abundance in ash generated by the Soufrière Hills volcano, Montserrat in the period 1997–2010. In: Wadge G, Robertson R, Voight B (eds) The eruption of Soufriere Hills volcano, Montserrat from 2000 to 2010. Geol Soc Lon Mem (in press)

Horwell CJ, Le Blond JS, Michnowicz SAK, Cressey G (2010) Cristobalite in a rhyolitic lava dome: evolution of ash hazard. Bull Volcanol 72:249–253

Horwell CJ, Sparks RSJ, Brewer TS, Llewellin EW, Williamson BJ (2003) The characterisation of respirable volcanic ash from the Soufriere Hills Volcano, Montserrat, with implications for health hazard. Bull Volcanol 65:346–362

Horwell CJ, Williamson BJ, Le Blond JS, Donaldson K, Damby DE, Bowen L (2012) The structure of volcanic cristobalite in relation to its toxicity; relevance for the variable crystalline silica hazard. Part Fibre Toxicol 9:44

Jones JB, Segnit ER (1972) Genesis of cristobalite and tridymite at low temperatures. J Geol Soc Aust 18(4):419–422

Kennedy LA, Russell JK, Nelles E (2009) Origins of Mount St. Helens cataclasites: experimental insights. Am Mineral 94:995–1004

Kingma KJ, Hemley RJ (1994) Raman spectroscopic study of microcrystalline silica. Am Mineral 79:269–273

Korzhinsky MA, Tkachenko SI, Shmulovich KI, Steinberg GS (1995) Native Al and Si formation. Nature 375(6532):544–544

Larsen ES, Irving J, Gonyer FA, Larsen ES (1936) Petrologic results of a study of the minerals from the Tertiary volcanic rocks of the San Juan region, Colorado. Part 2. Silica minerals. Am Mineral 21 (11):679–700

Le Blond JS, Cressey G, Horwell CJ, Williamson BJ (2009) A rapid method for quantifying single mineral phases in heterogeneous natural dust using X-ray diffraction. Powder Diffract 24:17–23

Lofgren G (1971) Experimentally produced devitrification textures in natural rhyolite glass. Geol Soc Am Bull 82:111–124

Martel C, Bourdier J-L, Pichavant M, Traineau H (2000) Textures, water content and degassing of silicic andesites from recent plinian and dome-forming eruptions at Mount Pelee volcano (Martinique, Lesser Antilles arc). J Volcanol Geotherm Res 96 (3–4):191–206

Matthews AJ, Barclay J, Carn S, Thompson G, Alexander J, Herd R, Williams C (2002) Rainfall-induced volcanic activity on Montserrat. Geophys Res Lett 29(13):1644

McBirney AR (1993) Igneous petrology. Jones & Bartlett, Boston

Mueller S, Melnik O, Spieler O, Scheu B, Dingwell DB (2005) Permeability and degassing of dome lavas undergoing rapid decompression: an experimental determination. Bull Volcanol 67:526–538

Murphy MD, Sparks RSJ, Barclay J, Carroll MR, Brewer TS (2000) Remobilization of andesite magma by intrusion of mafic magma at the Soufriere Hills volcano, Montserrat, West Indies. J Petrol 41 (1):21–42

Nakada S, Motomura Y (1999) Petrology of the 1991–1995 eruption at Unzen: effusion pulsation and groundmass crystallization. J Volcanol Geotherm Res 89(1–4):173–196

Nývlt J (1995) The Ostwald rule of stages. Cryst Res Technol 30 (4):443–449

Pallister JS, Thornber CR, Cashman KV, Clynne MA, Lowers HA, Mandeville CW, Brownfield IK, Meeker GP (2008) Petrology of the 2004–2006 Mount St. Helens lava dome—implications for magmatic plumbing and eruption triggering. In: Sherrod DR, Scott WE, Stauffer PH (eds) A volcano rekindled: the renewed eruption of Mount St. Helens, 2004–2006. U. S. Geological Survey Professional Paper, pp 647–702

Paterson MS, Wong T (2005) Experimental rock deformation—the brittle field. Springer-Verlag, Berlin, p 351

Pichavant M, Costa F, Burgisser A, Scaillet B, Martel C, Poussineau S (2007) Equilibration scales in silicic to intermediate magmas—implications for experimental studies. J Petrol 48(10):1955–1972

Reich M, Zúñiga A, Amigo A, Vargas G, Morata D, Palacios C, Parada MA, Garreaud RD (2009) Formation of cristobalite nanofibers during explosive volcanic eruptions. Geology 37(5):435–438

Renders PJN, Gammons CH, Barnes HL (1995) Precipitation and dissolution rate constants for cristobalite from 150 to 300 °C. Geochim Cosmochim Acta 59(1):77–85

Rogers AF (1922) A new occurrence of cristobalite in California. J Geol 30:211–216

Scheu B, Kueppers U, Mueller S, Spieler O, Dingwell DB (2008) Experimental volcanology on eruptive products of Unzen volcano. J Volcanol Geotherm Res 175(1–2):110–119

Scott JAJ, Pyle DM, Mather TA, Rose WI (2013) Geochemistry and evolution of the Santiaguito volcanic dome complex, Guatemala. J Volcanol Geotherm Res 252:92–107

Shmulovich KI, Yardley BWD, Graham CM (2006) Solubility of quartz in crustal fluids: experiments and general equations for salt solutions and H_2O–CO_2 mixtures at 400–800 °C and 0.1–0.9 GPa. Geofluids 6(2):154–167

Smith R, Sammonds PR, Tuffen H, Meredith PG (2011) Evolution of the mechanics of the 2004–2008 Mt St. Helens

lava dome with time and temperature. Earth Planet Sci Lett 307 (1–2):191–200

Sparks RSJ, Murphy MD, Lejeune AM, Watts RB, Barclay J, Young SR (2000) Control on the emplacement of the andesite lava dome of the Soufriere Hills Volcano by degassing-induced crystallization. Terra Nova 12:14–20

Spieler O, Kennedy B, Kueppers U, Dingwell DB, Scheu B, Taddeucci J (2004) The fragmentation threshold of pyroclastic rocks. Earth Planet Sci Lett 226(1–2):139–148

Stimac J, Hickmott D, Abel R, Larocque ACL, Broxton D, Gardner J, Chipera S, Wolff J, Gauerke E (1996) Redistribution of Pb and other volatile trace metals during eruption, devitrification, and vapor-phase crystallization of the Bandelier Tuff, New Mexico. J Volcanol Geotherm Res 73:245–266

Swanson SE, Naney MT, Westrich HR, Eichelberger JC (1989) Crystallization history of Obsidian Dome, Inyo Domes, California. Bull Volcanol 51:161–176

Voight B, Elsworth D (2000) Instability and collapse of hazardous gas-pressurized lava domes. Geophys Res Lett 27(1):1–4

Wadge G, Voight B, Sparks RSJ, Cole P, Loughlin SC, Robertson R (2013) An overview of the eruption of Soufrière Hills volcano from 2000–2010. In: Wadge G, Robertson R, Voight B (eds) The eruption of Soufriere Hills volcano, Montserrat from 2000 to 2010. Geol Soc Lon Mem (in press)

Watts RB, Herd RA, Sparks RSJ, Young SR (2002) Growth patterns and emplacement of the andesitic lava dome at Soufrière Hills Volcano, Montserrat. In: Druitt TH, Kokelaar BP (eds) The eruption of Soufrière Hills volcano, Montserrat, from 1995 to 1999. Geol Soc Lon Mem 21:115–152

White AF, Hochella MF (1992) Surface chemistry associated with the cooling and subaerial weathering of recent basalt flows. Geochim Cosmochimi Acta 56:3711–3721

Williamson BJ, Di Muro A, Horwell CJ, Spieler O, Llewellin EW (2010) Injection of vesicular magma into an andesitic dome at the effusive–explosive transition. Earth Planet Sci Lett 295:83–90

Yurtmen S, Rowbotham G (1999) A scanning electron microscope study of post-depositional changes in the northeast Nigde ignimbrites, South Central Anatolia, Turkey. Min Mag 63(1):131–141

Zellmer GF, Hawkesworth CJ, Sparks RSJ, Thomas LE, Harford CL, Brewer TS, Loughlin SC (2003) Geochemical evolution of the Soufrière Hills volcano, Montserrat, Lesser Antilles Volcanic Arc. J Petrol 44(8):1349–1374